Carboxy-terminal Determinants of Conductance in Inward-rectifier K Channels

Yu-Yang Zhang,[1] Janice L. Robertson,[2] Daniel A. Gray,[1] and Lawrence G. Palmer[1]

[1]Department of Physiology and Biophysics and [2]Graduate Program in Physiology, Biophysics, and Systems Biology, Weill Medical College of Cornell University, New York, NY 10021

ABSTRACT Previous studies suggested that the cytoplasmic COOH-terminal portions of inward rectifier K channels could contribute significant resistance barriers to ion flow. To explore this question further, we exchanged portions of the COOH termini of ROMK2 (Kir1.1b) and IRK1 (Kir2.1) and measured the resulting single-channel conductances. Replacing the entire COOH terminus of ROMK2 with that of IRK1 decreased the chord conductance at $V_m = -100$ mV from 34 to 21 pS. The slope conductance measured between −60 and −140 mV was also reduced from 43 to 31 pS. Analysis of chimeric channels suggested that a region between residues 232 and 275 of ROMK2 contributes to this effect. Within this region, the point mutant ROMK2 N240R, in which a single amino acid was exchanged for the corresponding residue of IRK1, reduced the slope conductance to 30 pS and the chord conductance to 22 pS, mimicking the effects of replacing the entire COOH terminus. This mutant had gating and rectification properties indistinguishable from those of the wild-type, suggesting that the structure of the protein was not grossly altered. The N240R mutation did not affect block of the channel by Ba^{2+}, suggesting that the selectivity filter was not strongly affected by the mutation, nor did it change the sensitivity to intracellular pH. To test whether the decrease in conductance was independent of the selectivity filter we made the same mutation in the background of mutations in the pore region of the channel that increased single-channel conductance. The effects were similar to those predicted for two independent resistors arranged in series. The mutation increased conductance ratio for Tl^+:K^+, accounting for previous observations that the COOH terminus contributed to ion selectivity. Mapping the location onto the crystal structure of the cytoplasmic parts of GIRK1 indicated that position 240 lines the inner wall of this pore and affects the net charge on this surface. This provides a possible structural basis for the observed changes in conductance, and suggests that this element of the channel protein forms a rate-limiting barrier for K^+ transport.

KEY WORDS: ROMK2 • IRK1 • GIRK1 • cytoplasmic pore • single-channel conductance

INTRODUCTION

K channels have high degrees of homology within the so-called "P-regions" and share the common motif T/S-x-G-Y-G which is thought to form the selectivity filter of the pore (Jan and Jan, 1990). Nevertheless single-channel conductances among K channels vary widely. For example, in the Ca-activated K channels values range from ~200 pS for BK ("maxi" K) channels to ~4 pS for some low-conductance Ca-activated K channels (Hille, 2001). Inwardly rectifying potassium (Kir) channels comprise an important family of channels that play roles in regulating membrane excitability, heart rate, hormone release, and renal K^+ secretion. The defining characteristic of Kir family members is that they conduct more effectively when the membrane potential is negative to E_k than when positive to E_k (Matsuda et al., 1987; Vandenberg, 1987; Ficker et al., 1994; Lopatin et al., 1994). Single-channel conductances also vary among the Kir channels, from ~50 fS (Kir 7) (Krapininsky et al., 1998) to ~75 pS (Kir6.2) (Shyng et al., 1997).

The structure of Kir channels, predicted from hydrophobicity plots and mutagenesis studies and later verified by the crystal structure of the bacterial inward rectifier KirBac1.1 (Kuo et al., 2003), consists of two hydrophobic segments spanning the membrane as α-helices (M1 and M2), an extracellular connecting segment containing the selectivity filter, and cytoplasmic NH_2 and COOH termini. As in other K channels, the selectivity filter and the M2 helices form the transmembrane pore. However it has also been shown that the COOH terminus of the channel is important for determining both rectification and conductance (Taglialatela et al., 1994, 1995; Yang et al., 1995; Choe et al., 2000; Kubo and Murata, 2001). Amino acids on the COOH terminus that control the inward rectification have been identified, including two negatively charged residues (E224 and E299 of Kir2.1) (Taglialatela et al., 1995; Yang et al., 1995; Kubo and Murata, 2001), but the determinants of conductance are still unknown.

Address correspondence to Lawrence G. Palmer, Department of Physiology and Biophysics, Weill Medical College of Cornell University, 1300 York Ave., New York, NY 10021. Fax: (212) 746-8690; email: lgpalm@med.cornell.edu

J. Gen. Physiol. © The Rockefeller University Press • 0022-1295/2004/12/729/11 $8.00
Volume 124 December 2004 729–739
http://www.jgp.org/cgi/doi/10.1085/jgp.200409166

Based on previous studies of ROMK, IRK, and various chimeras, we proposed a model of the Kir pore with two resistors in series (Choe et al., 2000). A component of the channel resistance conferred by its COOH terminus appeared to be additive with, and independent of, that of the extracellular loop or P-regions. In this paper, we seek to identify the components of the COOH terminus that comprise the "resistor" in series with the selectivity filter. These components are then mapped onto the structure of KirBac1.1 channel to investigate the physical basis of the series resistor.

MATERIALS AND METHODS

Chimera Constructions and In Vitro Mutagenesis

We engineered several chimeric channels in which parts of the COOH termini of ROMK2 (Zhou et al., 1994) and IRK1 (Kubo et al., 1993) were exchanged. The basic method for chimera construction was similar to that described previously (Choe et al., 1999). Our reference point was a chimera (C13) that is based on ROMK2 but has the COOH terminus of IRK1. We constructed additional chimeras in which the COOH-terminal IRK1 segment is progressively shorter as illustrated schematically in Fig. 1 A. The amino acids at which junctions between ROMK2 and IRK1 sequences occur were F232 for chm132, V275 for chm133, L301 for chm134, and V329 for chm135. Site-directed mutants were made using the Pfu enzyme (Stratagene) according to manufacturer's instructions. Primers were synthesized by Operon Technologies, Inc. Sequences of all the chimeras and point mutants were confirmed using an ABI 377XL automated DNA sequencer at The Cornell University Bio Resource Center.

Channel Expression

The plasmids were linearized with NotI restriction enzyme and cRNA's were transcribed with T7 RNA polymerase using mMESSAGE mMACHINE kit (Ambion). cRNA pellets were dissolved in nuclease-free water and stored in −70°C before use. Oocytes harvested from *Xenopus laevis* were incubated in OR2 solution with 2 mg/ml collagenase type II (Worthington) and 2 mg/ml hyaluronidase type II (Sigma-Aldrich) and incubated with gentle shaking for 60 min and another 30 min (if necessary) in a fresh enzyme solution at room temperature. Before the injection, oocytes were incubated in OR2 solution for 2 h under 19°C. Defolliculated oocytes were selected and injected with RNA. Following the injection, they were stored at 19°C in Leibovitz's L15 medium (Invitrogen) for 1–2 d before measurements were made.

Electrophysiology

Prior to patch clamping the oocyte, vitelline membrane was mechanically removed in a hypertonic solution containing 200 mM sucrose. Oocytes were bathed in a solution containing (in mM) KCl (110), $CaCl_2$ (2), $MgCl_2$ (1), and HEPES (5) at pH 7.4. When Tl^+ was the conducted ion, all but 2 mM Cl^- in the medium was replaced with NO_3^- to prevent precipitation of TlCl. Patch-clamp pipettes were prepared from Fisherbrand hematocrit capillary glass (Fisher Scientific) using a three-stage puller, coated with Sylgard® (Dow Corning) and fire polished with a microforge. Pipettes were filled with solution containing the same components as the bath solution; their resistances ranged from 1 to 5 MΩ.

Currents were recorded using a model 8900 patch-clamp amplifier (Dagan Corp.). Records were sampled at 50 kHz using an ITC-16 interface (Instrutech) and Pulse and Pulsefit software (HEKA Elektronik). For analysis, data were filtered at 1 kHz. Construction of open and closed time histograms and fitting with exponential distributions were performed using the TAC program (Bruxton Co.).

Whole-cell conductances were measured in intact oocytes using a two-electrode voltage clamp (OC-725; Warner Instrument Corp.). Intracellular pipettes had resistance of 0.5–1 MΩ when filled with 1 M KCl. Steady-state current–voltage relations were determined with the same extracellular bathing solution described above over a range of −120 to +80 mV with a holding potential of 0 mV. pH titration curves in intact oocytes were obtained by changing the extracellular pH with permeant acetate-buffered solutions to control intracellular pH (Tsai et al., 1995; Choe et al., 1997).

Modeling

Models of the GIRK1 (Kir3.1) cytoplasmic domain containing the ROMK2 (N) and IRK1 (R) mutation at position Q261 (of GIRK1) were generated from the tetrameric version of the GIRK1 crystal structure pdb file 1N9P (Nishida and MacKinnon, 2002). The pdb file was modified such that all selenomethionine residues were replaced with methionine. Using the biomolecular simulation program CHARMM version c31a0 (Brooks et al., 1983), the glutamine at position 261 was replaced with either asparagine or arginine by overlapping the side chains and keeping the same coordinates for similar atoms. The positions of the remaining atoms were generated from an internal coordinate table, and then the entire structure was relaxed with a short energy minimization. A potassium ion was then fixed in the plane of residue 161 and another energy minimization was performed to produce the final structure. The images of the molecular structures were generated using the program RasWin.

RESULTS

To identify regions of the cytoplasmic COOH terminus that affect ion permeation, we first extended the approach taken previously (Choe et al., 1999, 2000) using chimeras of Kir1.1 (ROMK2) and Kir2.1 (IRK1). The starting point was the chimera C13, which has the COOH terminus from IRK and the rest of the protein from ROMK2. We confirmed previous results showing that C13 has a single-channel conductance that is lower than that of ROMK2 (Fig. 1). We then extended the part of the channel coming from ROMK2 further into the COOH terminus. These constructs are shown schematically in Fig. 1 A.

When the ROMK2 part of the channel was extended to position V328 (C135) or to position L301 (C134), the conductance as well as the gating pattern and rectification characteristics were similar to those of ROMK2 itself. Typical traces are shown in Fig. 1 B, and I–V relationship for C135 is plotted in Fig. 1 C. These relationships are not precisely linear, with the slope conductance increasing at large negative voltages. Similar results were reported previously (Choe et al., 2000). Currents from these two chimeras superimposed on those from ROMK2 for voltages more positive than −100 mV. At larger negative voltages, C134 currents tended to be slightly larger. We therefore concluded

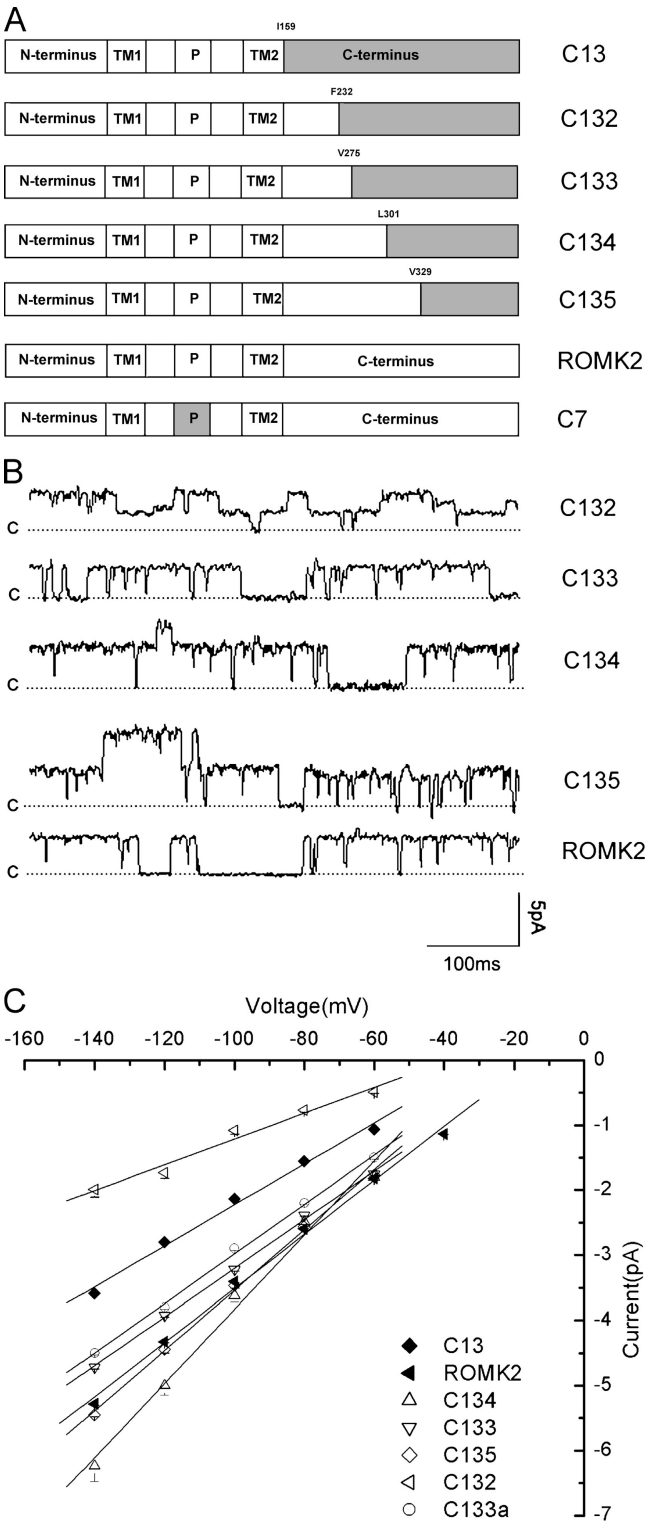

FIGURE 1. Single-channel conductance and ROMK2/IRK1 chimeras. (A) ROMK2/IRK1 chimeras. Parts of ROMK2 are white, and parts of IRK1 are shaded. Chimera C13 has the entire COOH terminus, probably including the last part of the second transmembrane domain (M2), from IRK1, and the rest of the channel from ROMK2. Other chimeras have progressively smaller portions of the COOH terminus from IRK1. (B) Inward current traces measured in the cell-attached configuration with a cell potential of −100 mV with respect to the pipette. The dotted lines indicate the closed state, with upward deflections indicating channel openings. (C) I–V relationships. Data represent means ± SEM for at least three different patches. A minimum of 15 transitions at each voltage were measured to obtain values for each patch. Slope conductances measured between −60 and −140 mV were ROMK2, 43 pS; C13, 31 pS; C132, 18 pS; C133, 37 pS; C133a, 38 pS; C134, 51 pS; and C135, 46 pS.

that the most distal parts of the COOH terminus do not have large effects on conductance, at least with respect to the decrease in current when the COOH terminus of ROMK2 is replaced by that of IRK1.

The chimera C133, in which the ROMK2 portion extends to position V275, had a conductance which was smaller than that of either ROMK2 or C134, particularly at large negative voltages, although still larger than that of C13. This suggests that parts of the channel between residues 275 and 301 may help confer the reduced single-channel conductance. However, the largest effects occurred when the ROMK2 portion was shortened to residue F232 (C132). This construct had a conductance even smaller than that of C13. The gating pattern of this chimera also lacked the characteristic fast closures seen with ROMK and the other COOH-terminal chimeras.

We therefore examined the region between positions 232 and 275 in more detail. Another chimera, named C133a in which the ROMK2 portion extended to position N256, behaved like C133 (Fig. 1), suggesting that positions 232–256 were the most important for the conductance change. We then examined point mutations at positions where the net charge on the amino acid side chain was different in the two channels. The mutants ROMK2 I252E, H255E, and N256D expressed well but had single-channel characteristics similar to those of ROMK2. However, the ROMK2 N240R mutation reduced the single-channel conductance considerably without markedly affecting gating behavior, as shown in Fig. 2. This position therefore appears to be important for ion permeation and contributes substantially to the effect of the COOH terminus on conductance. We also tested the converse mutation, C13 R240N, to see if the conductance was increased. Unfortunately this mutant did not express well and single-channel measurements could not be made.

We also investigated effects of mutations in the region between residues 275 and 301 of ROMK2. In this case, we were unable to identify an individual amino acid change that mimicked this behavior. However, a triple mutant of ROMK2 in which the sequence (286)SATC(289) was exchanged for the corresponding amino acids AMTT from IRK1 produced channels that expressed well, had kinetics similar to those of ROMK, and single-channel currents that were lower at

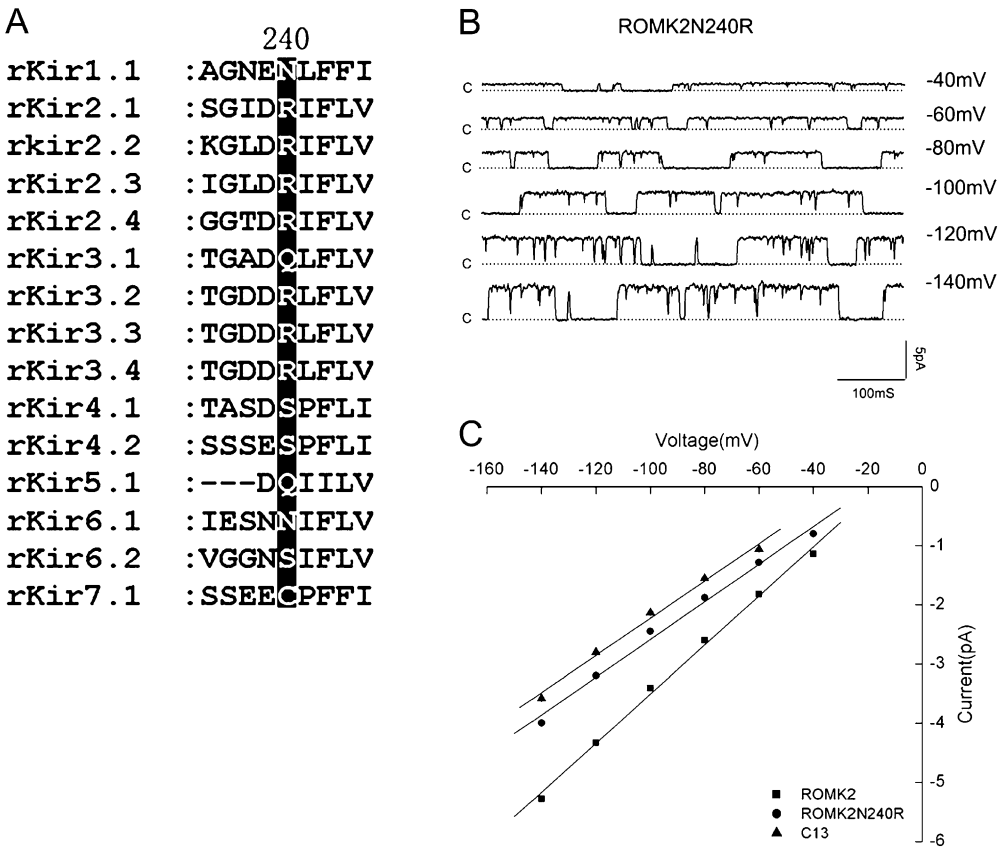

FIGURE 2. Single-channel conductance of the N240R mutation. (A) Alignment of the amino acid sequences of the rat K_{ir} channel family, showing sequence differences at positions N240. (B) Inward current traces for the mutant N240R measured in the cell-attached configuration with cell potentials of −40 to −140 mV. Dotted lines indicate the closed state and upward deflections indicate channel openings. (C) I–V relationships for N240R, N240K, and N240E, with data from ROMK2 and C13 shown for comparison. Data represent means ± SEM for at least three different patches. A minimum of 15 transitions at each voltage were measured to obtain values for each patch. The slope conductances measured between −60 and −140 mV were ROMK2, 43 pS; C13, 31 pS; and N240R, 31 pS.

large negative voltages (Fig. 3). Changes in this region therefore mimic the reduction in conductance seen with chimera C133. Again, the converse mutation on the C13 background did not express well. Combining this triple mutation with the N240R substitution produced channels with low conductance similar to the C132 chimera as well as a very low open probability. Because the effects of the triple mutation alone on conductance were small, and the combined mutant had altered gating properties, we did not investigate these constructs further.

The N240R phenotype was studied in detail. The basic kinetic signature of the mutant was quite similar to that of wild-type ROMK2 (Fig. 4). Open-time histograms were well described by a single exponential distribution with a time constant of 20–25 ms. Two distinct populations of closures can be discerned by eye. Closed-time histograms could be fit with two exponentials having time constants of ~1.5 and 50–100 ms, respectively. This is similar to the kinetic parameters reported previously for ROMK2 channels (Choe et al., 1998). In addition, the macroscopic current–voltage relationship shows the same time-independent currents, and the steady-state I–V curves were nearly linear for both the wild-type and mutant channels (Fig. 5). Finally, we examined whether the mutation affected inhibition of the channel by cytoplasmic acidification. The two-electrode voltage clamp was used to measure whole-cell currents during changes in extracellular pH in the presence of the weak acid acetate. Previous studies have shown that under these conditions, intracellular and extracellular pH change in parallel, and that the channels respond mainly to changes in the intracellular compartment (Tsai et al., 1995; Choe et al., 1997). The titration curve for the N240R mutant channels was identical to that of the wild-type channels (Fig. 6), indicating that the mutation did not affect the acid-sensing apparatus or the pH-dependent gate. Thus, as far as we can tell, the mutation does not appear to grossly alter the structure of the channel.

To test whether the alterations in the COOH-terminal were independent of the selectivity filter, we tested whether the sensitivity to Ba^{2+} block was altered by the N240R mutation. In KcsA channels, Ba^{2+} binds at the cytoplasmic end of the selectivity filter (Jiang and MacKinnon, 2000), and in ROMK and IRK, mutations at the V121 position close to this site alter both conductance and block (Zhou et al., 1996; Choe et al., 2000; Alagem et al., 2001), suggesting a similar interaction in this channel. We reasoned that if the N240R mutation influenced conductance through the selectivity filter, it might also alter the affinity for Ba^{2+} block. As shown in Fig. 7, the N240R mutation had no measurable effect on Ba^{2+} affinity of ROMK2. We also made the same mu-

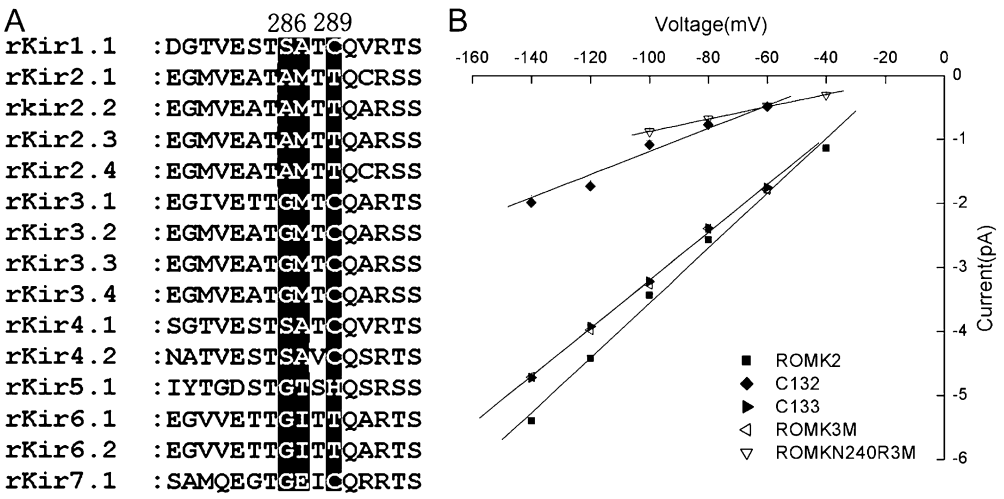

FIGURE 3. Effects of triple point mutations S286AA287M C289T (ROMK3M) on single-channel conductance of ROMK2. (A) Alignment of sequences of the Kir family in the region between residues 279 and 294 of ROMK2. (B) I–V relationships of ROMK2, C133 (in which the region in A is derived from IRK1), and the triple mutation S286AA287MC289T (ROMK3M) in which three of the residues of ROMK2 are mutated to the corresponding residues of IRK1, and the combined ROMK3M + N240R mutant. For comparison the I–V relationships of ROMK2 and C133 from Fig. 1 are superimposed. Slope conductances measured between −40 and −140 mV were ROMK2, 43 pS; C133, 37 pS; ROMK3M, 37 pS; ROMK3M N240R, 10 pS; C132, 18 pS.

tation on the background of the C7 chimera (Fig. 1), in which the P-regions of ROMK2 and IRK1 were exchanged. This involves changes in two amino acids at position 117 (L to I) and 121 (V to T). The C7 chimera itself had a higher affinity for Ba^{2+}, as reported previously (Zhou et al., 1996), but again, the N240R exchange did not alter block.

As a further test for the independence of the conductance properties conferred by the selectivity filter and the COOH terminus, we examined the effect of the N240R mutation on the C7 channels, which were found previously to have a single-channel conductance that is larger than that of ROMK2 itself, presumably due to an increase in conductance through the selec-

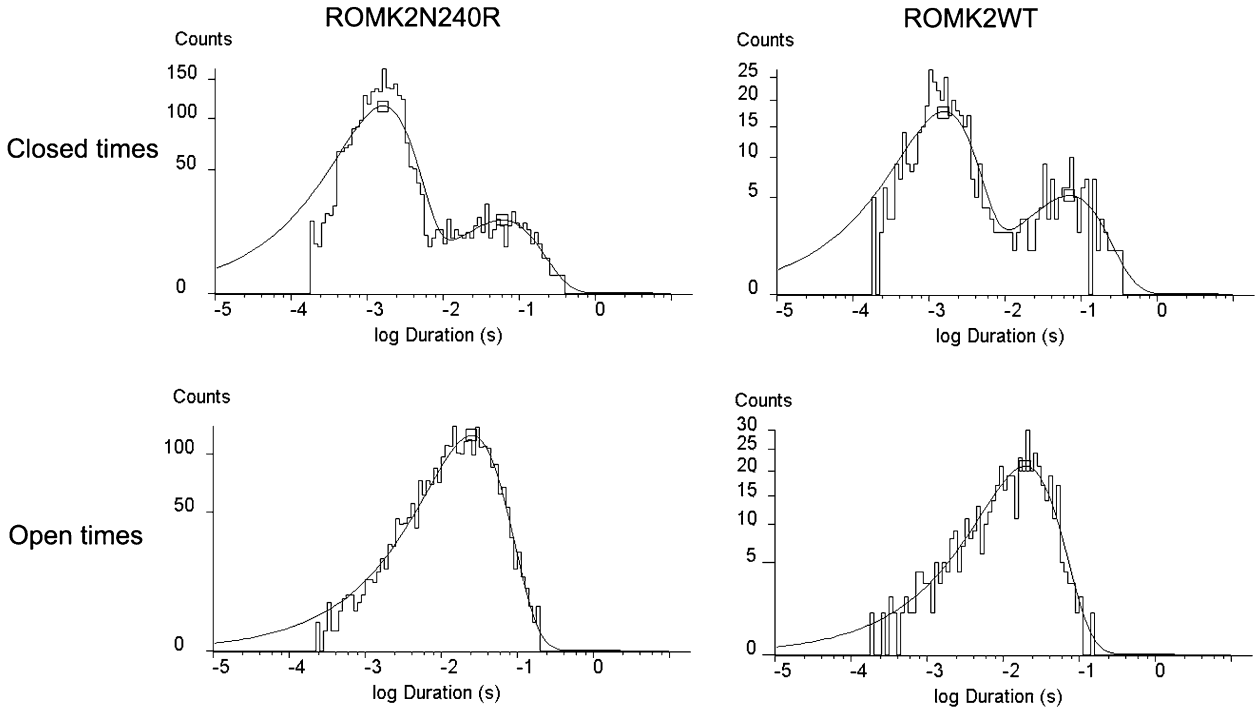

FIGURE 4. Kinetic properties of ROMK2 and ROMK2N240R. Currents were recorded from cell-attached patches containing only one channel at a cell potential of −100 mV. Above, closed-time histograms were fit with two exponentials. For ROMK2, the exponentials had time constants of 1.5 ms (77% of closures) and 70 ms (23%). For ROMK2N240R, the exponentials had time constants of 1.7 ms (87%) and 61 ms (13%). Below, open-time histograms were fit with one exponential distribution. Time constants were 20 ms for ROMK2 and 25 ms for N240R.

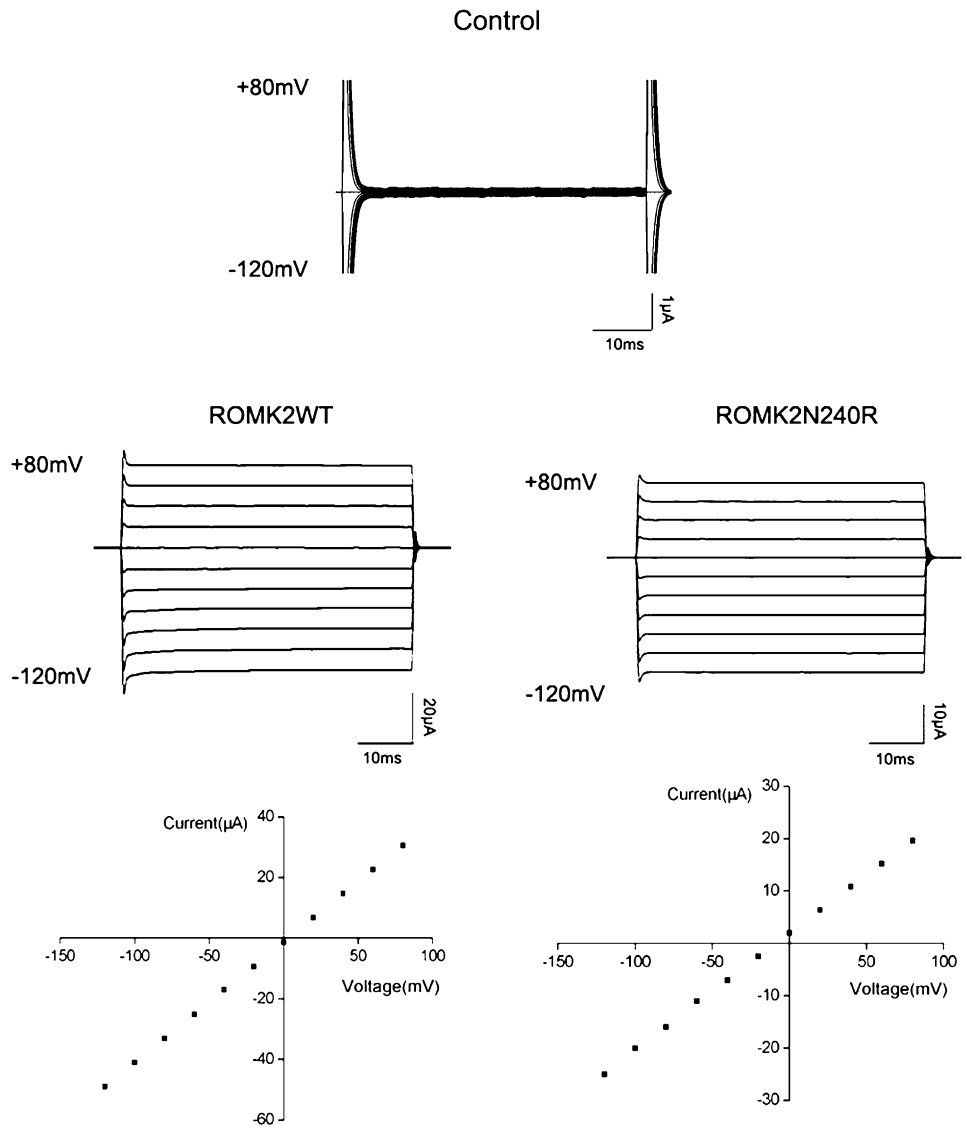

FIGURE 5. Macroscopic current–voltage relationships for ROMK2 and N240R. Above, current traces for an uninjected (control) oocyte. Steady-state currents were <200 nA. Middle, current traces measured with two-electrode voltage clamp in oocytes expressing ROMK2 and N240R. The extracellular K concentration was 110 mM. The membrane voltage was held at 0 mV and stepped to values between −120 and +80 mV for 50 ms. Below, steady-state I–V relationships.

tivity filter region (Choe et al., 2000). We reasoned that if the N240R mutation altered the conduction pathway independently of the selectivity filter, then the absolute reduction in single-channel conductance should, if anything, be larger in the C7 background. This prediction was confirmed as shown in Fig. 8. The slope conductance decreased from 58 pS for C7 to 36 pS for C7 N240R. More precisely, if the N240R mutation adds an additional barrier to ion movement that is independent of the selectivity filter, the resistance increase should be similar in both cases. Measuring resistance in the range of −40 to −100 mV, where the I–V curves are reasonably linear in all cases, we calculate that the N240R mutation increases resistance by 8.2 GΩ in the ROMK2 background and by 10.7 GΩ in the C7 background. We considered the two values to be in reasonable agreement. Thus, at least to a first approximation, the effects on conductance of changing the selectivity filter and the COOH terminus are independent.

To examine the mechanism of the effect of the N240R substitution on conductance, we tested for the role of a change in charge at this location. Substitution of K for N at position 240 also reduced the single-channel conductance, although to a lesser extent (Fig. 9). This suggests that both the size of the side chain as well as its charge affects the conductance. We also mutated N240 to E. The conductance was increased over that of ROMK2, although again the effect was smaller than that of the R substitution (Fig. 9). Finally, we mutated the neighboring E239 residue to Q to subtract a negative charge from this part of the channel. This decreased the conductance slightly from 43 to 39 pS (unpublished data). Although the change in the net charge was the same as that of the N240R mutation, the decrease in conductance was smaller. Therefore, the

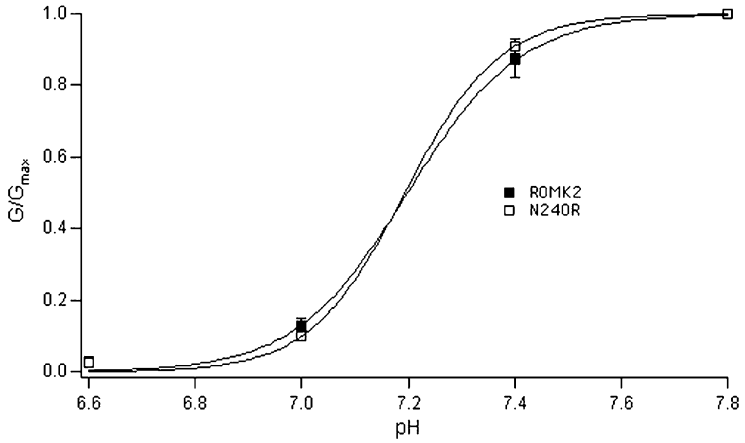

FIGURE 6. pH-dependence of macroscopic currents. Oocytes were bathed in solutions containing 55 mM Kacetate. The pH of the extracellular solution was reduced in steps, and the currents were measured after a new steady-state was achieved in 10–15 min. Inward conductance was normalized to maximal values measured at pH 7.8. Data points represent means ± SEM for four oocytes. Solid lines represent best fits to a Hill equation with pKa = 7.20 and n = 4.1 (ROMK) and pKa = 7.19 and n = 4.9 (N240R).

precise position of the mutation, as well as the changes in charge and size, is important.

We reported previously that substitution of the COOH terminus of IRK1 into ROMK2 altered the ion selectivity of the channel by increasing the conductance ratio for Tl^+:K^+ (Choe et al., 2000). The N240R mutation appears to account at least in part for this phenomenon. Fig. 10 shows single-channel records for ROMK2 WT and N240R channels with Tl^+ as the major charge carrier. There was very little difference in the magnitude of the currents for the two channels under these conditions. When compared with the results for K^+, these results indicate that the mutation increases the Tl^+:K^+ conductance ratio as did the COOH-terminal substitution.

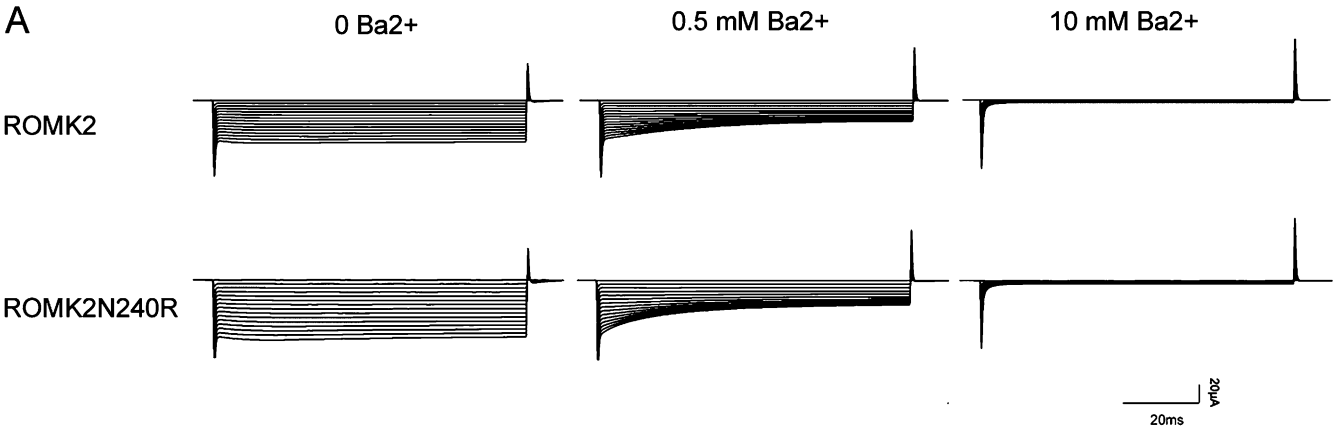

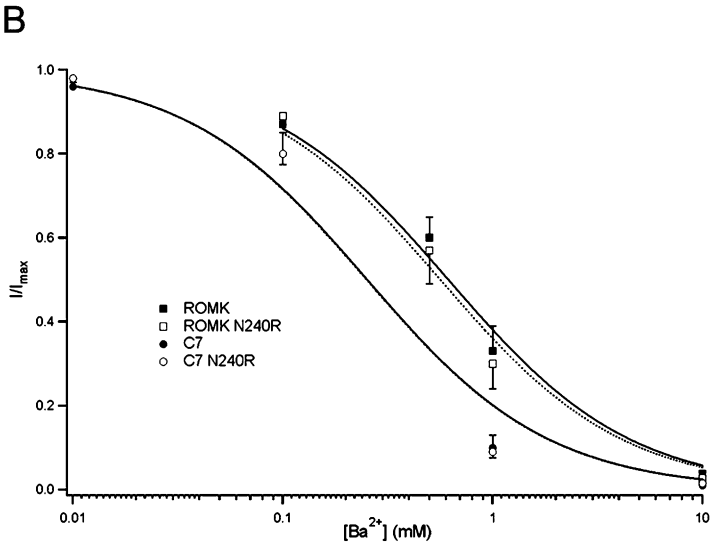

FIGURE 7. The N240R mutation does not affect Ba^{2+} block. Oocytes were superfused with solutions containing 110 mM KCl with and without added Ba^{2+}. Whole-cell currents were measured using the two-electrode voltage-clamp at voltages between 0 and −140 mV. (A) Typical current traces for ROMK2 and ROMK2 N240R with 0, 0.5, and 10 mM Ba^{2+}. (B) Currents at a test potential of −100 mV were normalized to their value in the absence of Ba^{2+} and plotted vs. Ba^{2+} concentration. Lines represent fits to a simple titration curve with K_i values of 0.62 mM (ROMK2), 0.56 mM (ROMK2 N240R), 0.25 mM (C7), and 0.25 mM (C7 N240R).

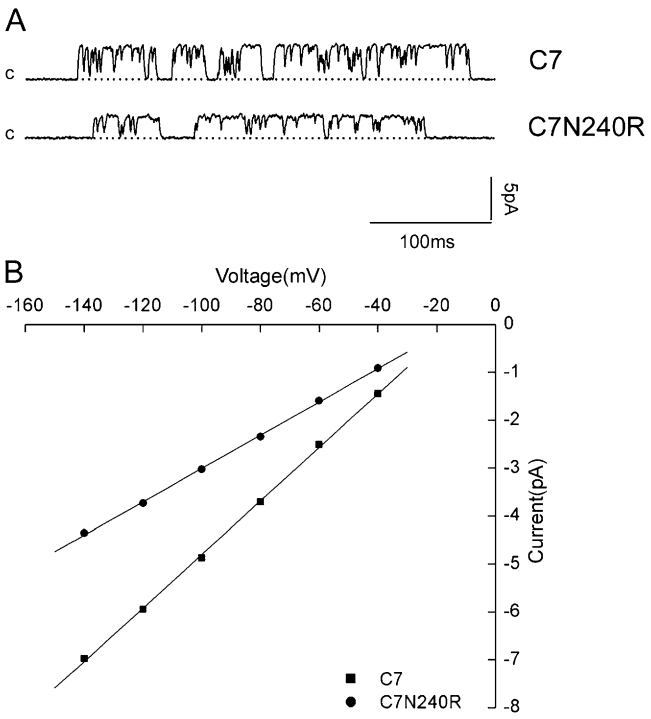

FIGURE 8. Effects of the N240R mutation on a channel with a higher conductance of the selectivity filter. (A) Single-channel traces for C7 chimera and C7 N240R with a holding potential of −80 mV. (B) I–V relationships for C7 and N240R. Single-channel conductances were C7, 58 pS, and C7 N240R, 36 pS.

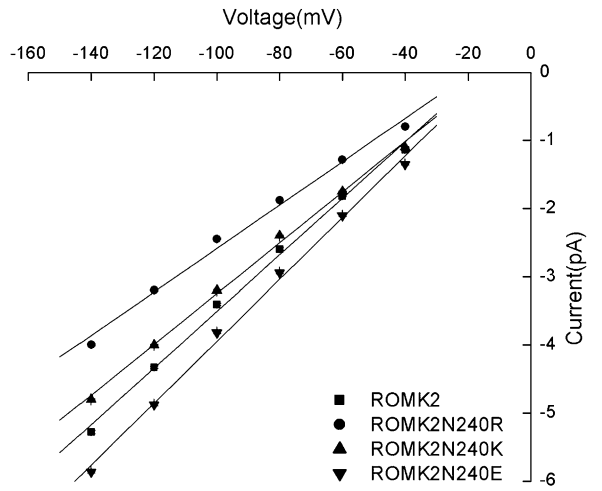

FIGURE 9. Effect of charge at position 240 on single-channel conductance. Conductances measured between −40 and −140 mV were ROMK2, 43 pS; C13, 31 pS; N240R, 31 pS; N240K, 37pS; and N240E, 45pS.

To further understand the structural basis of the conductance changes, we examined the location of our mutations with respect to the crystal structure of the cytoplasmic NH_2 and COOH termini of the GIRK1 (Kir3.1) channel (Nishida and MacKinnon, 2002). Fig. 11 A shows a side view of two subunits of the GIRK1 crystal structure. The residue Q261, corresponding to N240 of ROMK2, is highlighted using space-filling mode, and is located at the luminal surface of the pore near its cytoplasmic. Fig. 11 B shows an axial view of the model from the cytoplasm along the axis of the pore, in which the mutation to N (ROMK2) or R (IRK1) at residue Q261 has been made. The side chains of the mutant arginines protrude into the pore farther than in the case of the asparagine, and form a ring of positive charge around the conduction pathway. These models provide a plausible physical basis for the finding that both the size and charge of the side chain at position 240 in ROMK2 play a role in the changes of conductance.

DISCUSSION

The most important conclusion from these observations is that specific changes in amino acid side chains in the cytoplasmic part of Kir channels can influence the single-channel conductance. These effects can occur without changes in the gating or rectification properties of the channels, arguing against major structural changes. The simplest interpretation of these results is that these residues form part of the conducting pore, and that this part of the pore can confer significant resistance to the flow of ions.

The N240R mutation of ROMK2 appears to explain, at least in part, the decrease in single-channel conductance observed when the COOH terminus is exchanged for that of IRK1, as well as the change in selectivity for K^+ with respect to Tl^+. In a previous study, we found that the conductance changes conferred by exchanging the selectivity filter region and the COOH terminus were additive, and we postulated that these two parts of the protein effectively formed two resistors arranged in series (Choe et al., 2000). The present results support this conclusion. The decreased conductance due to N240R was exaggerated when the resistance of the selectivity filter was decreased in the C7 chimera. Furthermore the affinity of the pore for Ba^{2+} was unchanged by the COOH-terminal mutation. This parameter is quite sensitive to changes in or near the pore region (Zhou et al., 1996; Alagem et al., 2001). This suggests that the COOH terminus does not alter conductance through long-range effects on the selectivity filter.

Further support for this idea was provided by the recently determined crystal structures of the NH_2 and COOH termini of GIRK1 and of KirBac1.1 (Nishida and MacKinnon, 2002; Kuo et al., 2003), which suggest the basis for the cytoplasmic resistance. These structures form a channel that is wide enough to accommodate a K ion, but which might be small enough to impede the diffusion of the ions between the cytoplasm and the inner end of the transmembrane pore. One interpretation is that the cytoplasmic pore is an ob-

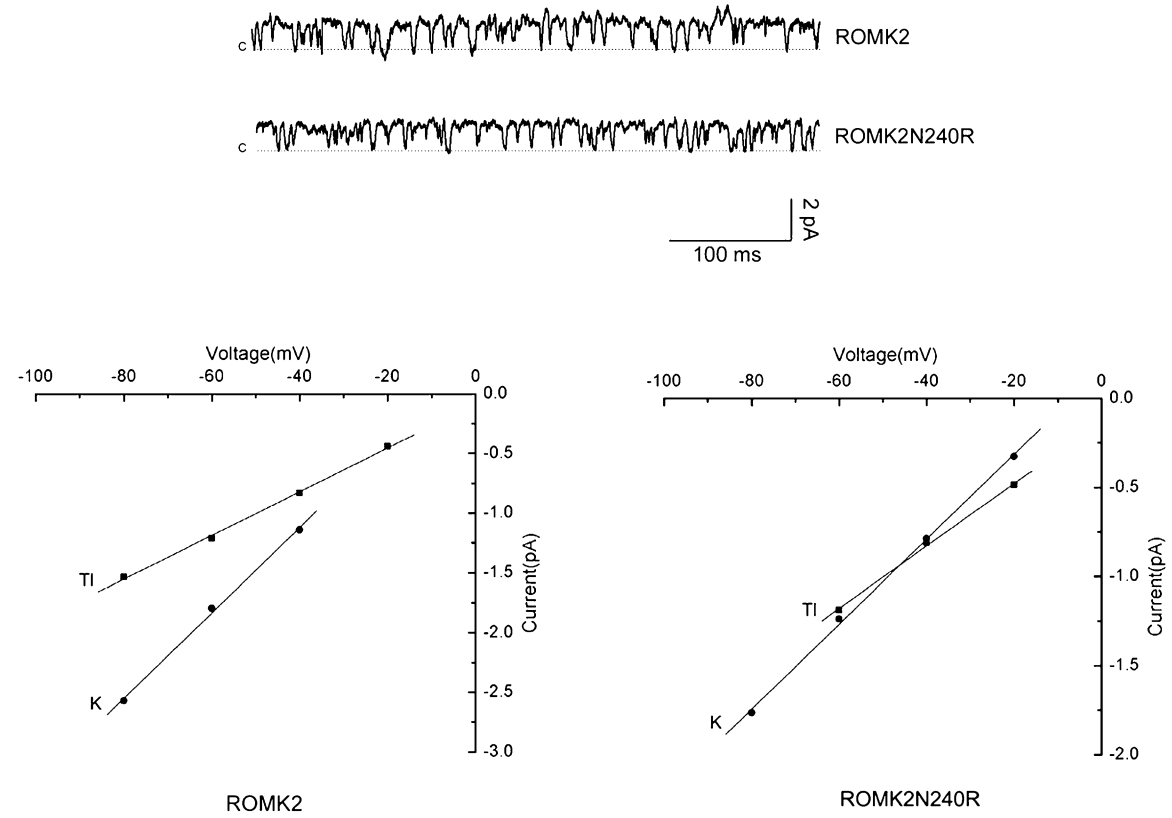

FIGURE 10. Tl^+ conductance and selectivity. Above, single-channel currents recorded in cell-attached patches with 110 mM Tl^+ in the pipette and a holding potential of −60 mV. Below: I-V relationships for K^+ and Tl^+ conductance in wild-type ROMK2 and N240R mutant channels. The single-channel conductances for Tl^+ were 18 pS in both channels. The Tl^+:K^+ conductance ratios were 0.51 for ROMK2 and 0.78 for N240R.

ligatory pathway in the conduction process, having a higher conductance in ROMK than in IRK1. Another possibility is that parallel pathways, which bypass the cytoplasmic pore, become more important, or even exclusive, routes for permeation in IRK1 or in the N240R mutant of ROMK2.

The N240 position does not correspond to the narrowest part of the GIRK cytoplasmic pore but lines a somewhat wider part further toward to the cytoplasmic end. This part of the pore becomes narrower when the critical amino acid is an arginine and the mutation adds four positive charges to the wall of the pore. The increase in net charge likely plays a role in reducing conductance, as putting a smaller positive charge at this position (N240K) also decreased conductance, and substituting a negative charge (N240E) increased. However, these effects were smaller than those of the N240R mutation, implying that charge is not the only factor involved, and that the size of the side chain is also important.

Other amino acids in the COOH terminus will certainly also affect ion permeation. Fig. 1 suggests that several parts of this part of the protein determine the open-channel conductance, and Fig. 3 highlights one of these regions. The N240R mutation is striking because it explains at least a significant part the effect of switching the COOH termini of ROMK2 and IRK1. This chimeric approach has the advantage that the substitutions involved are all natural ones in the sense that they occur in a related family member. A more complete description will probably require a scanning mutagenesis approach.

The specific residues identified here that account for the differences in single-channel conductance between ROMK2 and C13 are distinct from those in the COOH-terminal that confer rectification properties. The C13 chimera lacks the negatively charged aspartate in the lower part of TM2, which can itself confer inward rectification (Fakler et al., 1994; Lu and MacKinnon, 1994; Stanfield et al., 1994; Wible et al., 1994). It does however contain two glutamate residues (E299 and E224) in the COOH terminus, which also contribute to the rectification process (Taglialatela et al., 1995; Yang et al., 1995; Kubo and Murata, 2001). Neither the N240R mutation nor the triple mutation at the apex of the cytoplasmic pore affect the ratio of inward to outward currents. Mutation of E224 in IRK1 to G, the corresponding amino acid in ROMK2, decreased single-channel conductance (Taglialatela et al., 1995; Yang et

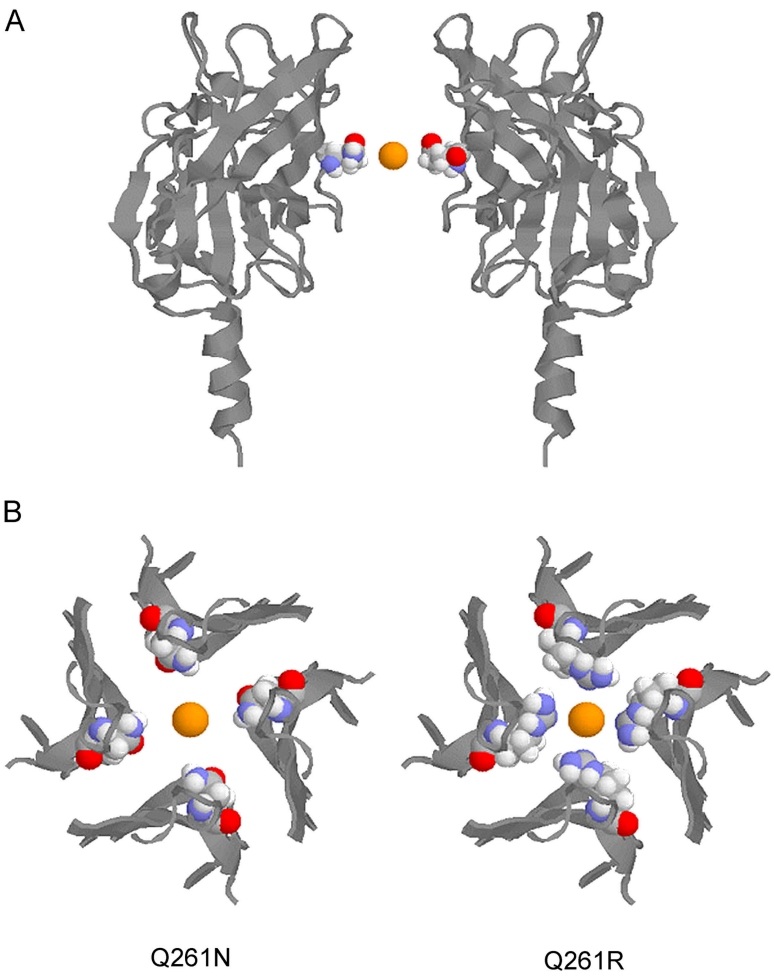

FIGURE 11. Model of the effect of N to R substitution in the cytoplasmic pore based on the crystal structure of GIRK1. (A) A side view of the crystal structure of the cytoplasmic domain of GIRK1-Kir3.1 (pdb:1N9P) is shown from the side with two subunits removed for clarity. Residue Q261, corresponding to residue R260 in IRK1-Kir2.1 and N240 in ROMK2-Kir1.1 is highlighted using space-filling mode along with a potassium ion in the same plane and centered along the pore axis. (B) Models of the GIRK1 cytoplasmic domain in which residue Q261 has been mutated to asparagine (left) or arginine (right) are shown here. A cytoplasmic view of the pore-lining residues 223–230, 253–264, and 298–311 is represented with cartoon rendering except for residue 261, which is highlighted using space-filling mode. A potassium ion is shown along the central axis and in the plane of residue 261.

al., 1995; Kubo and Murata, 2001). The interpretation of this finding is complicated, however, by an increase in open-channel noise in the E224G mutant. Thus the determinants of ion conduction and polyamine block may overlap but are not identical.

We propose that variation in single-channel conductance among the inward-rectifier channels is determined in part by differences in the conductance of the cytoplasmic pore formed primarily by the COOH terminus. These appear to be independent of differences due to the selectivity filter region, which can also affect single-channel conductance (Choe et al., 2000). The relative conductances or resistances of the selectivity filter and the cytoplasmic pore will therefore vary considerably from channel to channel. We further suggest that movement of ions through the cytoplasmic pore is a major pathway for ion permeation, at least through ROMK channels, and that the resistance of this pore is larger in IRK1.

We thank Benoit Roux for making the CHARMM software and computational facilities available to us.

This work was supported by National Institutes of Health grant DK27847.

Colin G. Nichols served as editor.

Submitted: 11 August 2004
Accepted: 20 October 2004

REFERENCES

Alagem, N., M. Dvir, and E. Reuveny. 2001. Mechanism of Ba^{2+} block of a mouse inwardly rectifying K^+ channel: differential contribution by two discrete residues. *J. Physiol.* 534:381–393.

Brooks, B.R., R.E. Bruccoleri, B.D. Olafson, D.J. States, S. Swaminathan, and M. Karplus. 1983. CHARMM: a program for macromolecular energy, minimization, and dynamics calculations. *J. Comp. Chem.* 4:187–217.

Choe, H., L.G. Palmer, and H. Sackin. 1999. Structural determinants of gating in inward-rectifier K^+ channels. *Biophys. J.* 76: 1988–2003.

Choe, H., H. Sackin, and L.G. Palmer. 1998. Permeation and gating of an inwardly rectifying potassium channel. Evidence for a variable energy well. *J. Gen. Physiol.* 112:433–446.

Choe, H., H.S. Sackin, and L.G. Palmer. 2000. Permeation properties of inward-rectifier potassium channels and their molecular determinants. *J. Gen. Physiol.* 115:391–404.

Choe, H., H. Zhou, L.G. Palmer, and H. Sackin. 1997. A conserved cytoplasmic region of ROMK modulates pH sensitivity, conductance, and gating. *Am. J. Physiol.* 273:F516–F529.

Fakler, B., U. Brandle, C.H. Bond, E. Glowatzke, C. Konig, J.P. Adelman, H.P. Zenner, and J.P. Ruppersberg. 1994. A structural determinant of differential sensitivity of cloned inward rectifier K^+

channels to intracellular spermine. *FEBS Lett.* 356:199–203.
Ficker, E., M. Taglialatela, B.A. Wible, C.M. Henley, and A.M. Brown. 1994. Spermine and spermidine as gating molecules for inward rectifier K^+ channels. *Science.* 266:1068–1072.
Hille, B. 2001. Ionic Channels of Excitable Membranes. 3rd ed. Sinauer Associates, Sunderland, MA. 814 pp.
Jan, L.Y., and Y.N. Jan. 1990. A superfamily of ion channels. *Nature.* 345:672.
Jiang, Y., and R. MacKinnon. 2000. The barium site in a potassium channel by x-ray crystallography. *J. Gen. Physiol.* 115:269–272.
Krapininsky, G., I. Medina, L. Eng, L. Krapivinsky, Y. Yang, and D. Clapham. 1998. A novel inward rectifier K^+ channel with unique pore properties. *Neuron.* 20:995–1005.
Kubo, Y., T.J. Baldwin, Y.N. Jan, and L.Y. Jan. 1993. Primary structure and functional expression of a mouse inward rectifier potassium channel. *Nature.* 362:127–133.
Kubo, Y., and Y. Murata. 2001. Control of rectification and permeation by two distinct sites after the second transmembrane domain region in Kir2.1 K^+ channel. *J. Physiol.* 531:645–660.
Kuo, A., J.M. Gulbis, J.F. Antcliff, T. Rahman, E.D. Lowe, J. Zimmer, J. Cuthbertson, F.M. Ashcroft, T. Ezaki, and D.A. Doyle. 2003. Crystal structure of the potassium channel KirBac1.1 in the closed state. *Science.* 300:1922–1926.
Lopatin, A.N., E.N. Makhina, and C.G. Nichols. 1994. Potassium channel block by cytoplasmic polyamines as the mechanism of intrinsic rectification. *Nature.* 372:366–369.
Lu, Z., and R. MacKinnon. 1994. Electrostatic tuning of Mg^{2+} affinity in an inward-rectifier K^+ channel. *Nature.* 371:243–246.
Matsuda, H., A. Saigusa, and H. Irisawa. 1987. Ohmic conductance through the inwardly rectifying K channel and blocking by internal Mg^{2+}. *Nature.* 325:156–159.
Nishida, M., and R. MacKinnon. 2002. Structural basis of inward rectification: cytoplasmic pore of the G protein-gated inward rectifier Girk1 at 1.8 Å resolution. *Cell.* 111:957–965.
Shyng, S.-L., T. Ferrigni, and C.G. Nichols. 1997. Control of rectification and gating of cloned KATP channels by the Kir6.2 subunit. *J. Gen. Physiol.* 110:141–153.
Stanfield, P.R., N.W. Davies, P.A. Shelton, M.J. Sutcliffe, I.A. Khan, W.J. Brammar, and E.C. Conley. 1994. A single aspartate residue is involved in both intrinsic gating and blockage by Mg^{2+} of the inward rectifier IRK1. *J. Physiol.* 478:1–6.
Taglialatela, M., E. Ficker, B.A. Wible, and A.M. Brown. 1995. C-terminus determinants for Mg^{2+} and polyamine block of the inward rectifier K^+ channel IRK1. *EMBO J.* 14:5532–5541.
Taglialatela, M., B.A. Wible, R. Caporaso, and A.M. Brown. 1994. Specification of pore properties by the carboxyl terminus of inwardly rectifying K^+ channels. *Science.* 264:844–847.
Tsai, T.D., M.E. Shuck, D.P. Thompson, M.J. Bienkowski, and K.S. Lee. 1995. Intracellular H^+ inhibits a cloned rat kidney outer medulla K^+ channel expressed in *Xenopus* oocytes. *Am. J. Physiol.* 268:C1173–C1178.
Vandenberg, C.A. 1987. Inward rectification of a potassium channel in cardiac ventricular cells depends on internal magnesium ions. *Proc. Natl. Acad. Sci. USA.* 84:2560–2564.
Wible, B.A., M. Taglialatela, E. Ficker, and A.M. Brown. 1994. Gating of inwardly rectifying K^+ channels localized to a single negatively charged residue. *Nature.* 371:246–249.
Yang, J., Y.N. Jan, and L.Y. Jan. 1995. Control of rectification and permeation in residues in two distinct domains in an inward rectifier K^+ channel. *Neuron.* 14:1047–1054.
Zhou, H., S. Chepilko, W. Schutt, H. Choe, L.G. Palmer, and H. Sackin. 1996. Mutations in the pore region of ROMK enhance Ba^{2+} block. *Am. J. Physiol.* 271:C1949–C1956.
Zhou, H., S.S. Tate, and L.G. Palmer. 1994. Primary structure and functional properties of an epithelial K channel. *Am. J. Physiol.* 266:C809–C824.